Atmospheric fate of two relevant unsaturated ketoethers: kinetics, products and mechanisms for the reaction of hydroxyl radicals with (*E*)-4-methoxy-3-buten-2-one and (1*E*)-1-methoxy-2-methyl-1-penten-3-one.

Rodrigo Gastón Gibilisco*[a], Ian Barnes[a†], Iustinian Gabriel Bejan*[b], Peter Wiesen[a]

[a]*Bergische Universität Wuppertal, Institute for Atmospheric and Environmental Research, 42097 Wuppertal / Germany*.
[b]*Faculty of Chemistry and Integrated Center of Environmental Science Studies in the North East Region - CERNESIM, "Al. I. Cuza" University, Iasi, Romania*

Abstract

The kinetics of the gas-phase reactions of hydroxyl radicals with two unsaturated ketoethers (UKE) at (298 ± 3) K and 1 atm of synthetic air have been studied for the first time using the relative rate technique in an environmental reaction chamber by in situ FTIR spectrometry. The rate coefficients obtained using propene and isobutene as reference compounds were (in units of 10^{-10} cm^3 $molecule^{-1}$ s^{-1}) as follows: k_{TMBO}(OH + (*E*)-4-methoxy-3-buten-2-one) = (1.41 ± 0.11), and k_{MMPO}(OH + (1*E*)-1-methoxy-2-methyl-1-penten-3-one) = (3.34± 0.43). In addition, quantification of the main oxidation products in the presence of NO_x has been performed and degradation mechanisms for these reactions were developed. Methyl formate, methyl glyoxal, PAN and PPN were identified as main reaction products and quantified for both reactions. The results of the present study provide new insights regarding the contribution of these multifunctional VOCs in the generation of secondary organic aerosols (SOAs) and long-lived nitrogen containing compounds in the atmosphere. Atmospheric lifetimes and implications are discussed in light of the obtained results.

Keywords: (*E*)-4-methoxy-3-buten-2-one, (1*E*)-1-methoxy-2-methyl-1-penten-3-one, OH radical kinetic, tropospheric chemistry, gas phase degradation mechanism, biomass burning, PAN and carbonyl formation.

* Corresponding authors.

E-mail address:

gibilisco@uni-wuppertal.de (R. G. Gibilisco)

iustinian.bejan@uaic.ro (I. Bejan)

†Deceased 1 January 2018

1. Introduction

Oxygenated volatile organic compounds (OVOCs) are ubiquitous atmospheric constituents of anthropogenic and natural origin. From those OVOCs, carbonyls have both direct and indirect sources, as a result of biogenic and anthropogenic activities, and because they are formed during chemical degradation processes, which occur in the atmosphere. Unsaturated carbonyls present high reactivity and are easily decomposed throughout chemical reactions into various OVOCs products.

Ketones are one of the dominant groups of carbonyls found in the lower troposphere. They can be emitted into the atmosphere by anthropogenic activities from industry, combustion engine vehicle exhaust and in a large extent are formed as reaction products of other VOCs in the troposphere (Calvert et al., 2011; Jiménez et al., 2014; Mellouki et al., 2015).

More complex unsaturated carbonyls, namely the α, β–unsaturated ketones and α, β-unsaturated ethers are either emitted by plants or are produced as a result of atmospheric oxidation of conjugated dienes (Lv et al., 2018; Mellouki et al., 2015; Zhou et al., 2006). These compounds have been considered as precursors for SOAs (Calvert et al., 2011).

α, β-unsaturated ketoethers are compounds with high structural complexity found in the atmosphere. They were detected as reaction products of the atmospheric degradation of furans and unsaturated ethers, compounds, which received substantial interest in the last decade since they are considered promising alternative fuels (Cilek et al., 2011; Li et al., 2018; Villanueva et al., 2009; Zhou et al., 2006). UKEs are also produced during combustion and more specifically in biomass burning (Hatch et al., 2015). They are also of great interest in the pharmaceutical industry since they are often used as precursors and/or intermediates in the production of new anticancer drugs (Gøgsig et al., 2012; Kumar et al., 2016).

α, β -unsaturated ketoethers are a special type of olefins, with an electron rich π system, which makes them more susceptible to rapid oxidation by addition of the OH radical to the double bond. Secondary pollutants, which are formed in such a reaction sequence, could be even more harmful than primary pollutants emitted into the atmosphere. Examples of such secondary harmful pollutants are organic peroxynitrates, highly oxidized molecules and SOAs (Atkinson, 2000; Calvert et al., 2015).

Accordingly, it is important to study in detail how the OH radical initiated oxidation of these compounds can affect the chemical composition and reactivity of the troposphere and, furthermore, the impact of the secondary pollutants formed during their gas phase chemical degradation.

In the present work the OH radical initiated reactions of (1*E*)-1-methoxy-2-methyl-1-penten-3-one and (*E*)-4-methoxy-3-buten-2-one have been investigated:

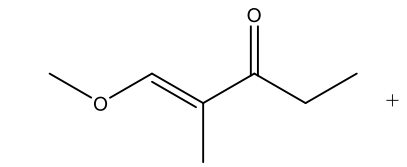

(1*E*)-1-methoxy-2-methyl-1-penten-3-one
MMPO

(1)

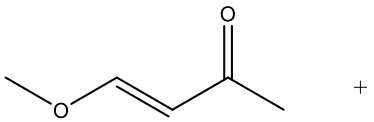

(*E*)-4-methoxy-3-buten-2-one
TMBO

(2)

In addition to the kinetic information, the gaseous reaction products of reactions (1) and (2) have been quantified and reaction mechanisms have been derived for both compounds. The present study represents the first experimental determination of the rate coefficients (k_{TMBO} and k_{MMPO}) and the reaction products formed from the gas phase reactions in the

presence of NO_x. The obtained results could be used to generate more complete atmospheric chemical degradation mechanisms, i.e. the master chemical mechanism, which is necessary for a better estimation of the contribution of such compounds to photooxidant and SOAs formation.

2. Experimental

All experiments were performed in a 1080 L quartz-glass reaction chamber at (298 ± 3) K and a total pressure of (760 ± 10) Torr of synthetic air. A pumping system consisting of a turbo-molecular pump backed by a double stage rotary fore pump was used to evacuate the reactor to 10^{-3} Torr. Three magnetically coupled Teflon mixing fans are mounted inside the chamber to ensure homogeneous mixing of the reactants. The photolysis system consists of 32 superactinic fluorescent lamps (Philips TL05 40W: 290–480 nm, λ_{max}= 360 nm) and 32 low-pressure mercury vapor lamps (Philips TUV 40W; λ_{max} = 254 nm), which are spaced evenly around the reaction vessel. The lamps are wired in parallel and can be switched individually, which allows variation of the light intensity, and thus also the photolysis frequency/radical production rate, within the chamber. The chamber is equipped with a White type multiple-reflection mirror system with a base length of (5.91 ± 0.01) m for sensitive in situ long path infrared absorption monitoring of reactants and products in the spectral range 4000 – 700 cm^{-1}. The White system was operated at 82 traverses, giving a total optical path length of (484.7 ± 0.8) m. Infrared spectra were recorded with a spectral resolution of 1 cm^{-1} using a Nicolet Nexus FTIR spectrometer equipped with a liquid nitrogen cooled mercury-cadmium-telluride (MCT) detector.

OH radicals were generated by photolysis of CH_3ONO/air mixtures at 360 nm using fluorescent lamps:

$CH_3ONO + h\nu \rightarrow CH_3O + NO$ (3)

$CH_3O + O_2 \rightarrow CH_2O + HO_2$ (4)

$HO_2 + NO \rightarrow OH + NO_2$ (5)

Quantification of TMBO and MMPO and gas phase products was performed by comparison with calibrated reference spectra contained in the IR spectral data bases of the Wuppertal laboratory.

To investigate the mechanism of the OH-radical initiated oxidation of the α, β–unsaturated ketoethers, the mixtures of the compound, CH_3ONO and air were irradiated for periods of 10-30 minutes during which infrared spectra were recorded with the FTIR spectrometer. Typically, up to 128 interferograms were co-added per spectrum over a period of approximately 40 s and 15-20 such spectra were collected. Prior to the reaction initiated by OH radicals, 5 spectra have been collected in dark to check the homogeneity and unexpected dark decay of the compounds under investigations (e.g. wall losses; dark reactions).

The TMBO, MMPO and reference compounds were monitored at the following infrared absorption frequencies (in cm^{-1}): TMBO at 958, 1253 and 3020, MMPO at 1245, 1653 and 2850, isobutene at 3085 and propene at 3091.

Rate coefficients for the reactions of OH radicals with MMPO and TMBO were determined by comparing their decay rate with that of the corresponding decay of the two reference compounds, isobutene and propene:

OH + UKE → Products (6)

OH + reference → Products (7)

Provided that the reference compound and TMBO and MMPO are lost only by reactions (6) and (7), it can be shown that:

$$ln\left\{\frac{[UKE]0}{[UKE]t}\right\} = \frac{k_{UKE}}{k_{reference}}\ ln\left\{\frac{[reference]0}{[reference]t}\right\} \quad \text{(I)}$$

where, $[UKE]_0$, $[reference]_0$, $[UKE]_t$ and $[reference]_t$ are the concentrations of the α, β-unsaturated ketoethers and the reference compound at times t=0 and t, respectively, and k_{UKE} and $k_{reference}$ are the rate coefficients of reactions (6) and (7), respectively.

The initial mixing ratios of the reactants in ppmV (1 ppmV = 2.46×10^{13} molecule cm^{-3} at 298 K and 1 atm) were TMBO (1-3), MMPO (2-4), isobutene (3-5) and propene (3-5). Methyl nitrite (6 ppmv) photolysis has been used for OH radical formation. No additional NO has been introduced in the reaction chamber.

Possible additional losses due to interferences and/or interactions with the reactor walls could be neglected or corrected. To verify this assumption, mixtures of CH_3ONO/air with the α, β–unsaturated ketoethers and the reference compound were prepared and allowed to stand in the dark for two hours. In all cases, the decay of the organic species in the presence of the OH radical precursor and in the absence of UV light was negligible. Furthermore, to test for a possible photolysis of the compounds, the reactant mixtures without OH radical precursor were irradiated for 30 minutes, using all lamps surrounding the chamber. No significant photolysis of any of the reactants was observed and no additional decay has been monitored due to a possible reaction with interfering radicals.

3. Materials

The following chemicals, with purities as stated by the supplier, were used without further purification: synthetic air (Air Liquide, 99.999%), propene (Messer Schweiz AG, 99.5%), isobutene (Messer, 99%), (*E*)-4-methoxy-3-buten-2-one technical grade (Aldrich, 90%) and (1*E*)-1-methoxy-2-methyl-1-penten-3-one (Aldrich, > 89.5 %). Methyl nitrite was prepared by the drop-wise addition of 50% sulfuric acid to a saturated solution of sodium

nitrite in water and methanol (Taylor et al., 1980). The products were carried by a stream of nitrogen gas through a saturated solution of sodium hydroxide followed by calcium chloride, to remove the excess of acid, water and methanol, respectively. Methyl nitrite was collected and stored at 193 K in dry ice.

4. Results and Discussion

4.1 Rate coefficients for the reaction with OH radicals

Plots of the kinetic data obtained from the experiments of the reaction of OH radicals with TMBO and MMPO using two different reference compounds are shown in Fig. 1 and 2, respectively. At least two experiments have been performed for each reference compound and linear plots were obtained in all cases. For better representation, data for all experiments have been plotted against both references. Rate coefficient ratio $k_{UKE}/k_{Reference}$ ($\pm 2\sigma$) obtained by combining the experiments results in Fig. 1 and Fig. 2 were: for TMBO, $k_{TMBO}/k_{isobutene} = (2.56 \pm 0.13)$ and $k_{TMBO}/k_{propene} = (5.08 \pm 0.16)$. For MMPO, $k_{MMPO}/k_{isobutene} = (6.40 \pm 0.31)$ and $k_{MMPO}/k_{propene} = (11.64 \pm 0.82)$.

The linearity of the plots with near-zero intercepts confirms that no interferences have affected the rate coefficient determination. Additionally, the very good agreement of the rate coefficients using the two reference compounds proved the correctness of the investigations.

Table 1 lists the values of the rate coefficient ratio $k_{UKE}/k_{Reference}$ obtained in the individual experiments at 298 K and 1 atm for each α, β–unsaturated ketoether. The errors given for the $k_{UKE}/k_{reference}$ ratios are the 2σ statistical errors from the linear regression. The rate coefficients k_{UKE} for reactions 1 and 2 were calculated using the recommended values $k_{propene} = (2.90 \pm 0.10) \times 10^{-11} cm^3$ molecule^{-1} s^1(Atkinson et al., 2006) (OH +

propene) and $k_{isobutene}$= (5.23 ± 0.24) × $10^{-11}$$cm^3$ $molecule^{-1}$ s^1 (OH + isobutene) (Atkinson and Aschmann, 1984).

In addition, Table 1 shows the rate coefficients for individual experiments of each reference compound employed in this study as well as the final quoted rate coefficients for the reactions of OH with UKE compounds as an average from all experimental values obtained for the corresponding compound. The error quoted for those final UKE rate coefficients are obtained by using an error propagation approach.

To the best of our knowledge rate coefficients for the reactions of OH radicals with (*E*)-4-methoxy-3-buten-2-one and (1*E*)-1-methoxy-2-methyl-1-penten-3-one have not been reported previously in the literature.

4.1.1Reactivity trends

There is a general lack of studies on the reactivity of poly-substituted oxygenated unsaturated compounds, such as the unsaturated ketoethers studied in this work.

Only the reactivity of (*E*)-4-methoxy-3-buten-2-one towards ozone was investigated by Grosjean and Grosjean (1999) who reported a rate coefficient k_{O3} of 1.3 × 10^{-16} cm^3 $molecule^{-1}$ s^{-1} (Grosjean and Grosjean, 1999). The authors identified and quantified two main products from the ozonolysis of (*E*)-4-methoxy-3-buten-2-one, namely methylglyoxal (31.2 ± 1.9%) and methyl formate (> 15.7%). These two species are potential products of the OH-initiated oxidation of (*E*)-4-methoxy-3-buten-2-one as well.

It is well known that OH-initiated atmospheric degradation of unsaturated VOCs proceeds mainly through the addition of the OH radical to the double bond (Calvert et al., 2015). Some studies also suggested that the presence of oxygenated functional groups in unsaturated VOCs leads to an increase of k_{OH}, perhaps due to the possibility of hydrogen bonding transition complexes stabilizing the transition states involved in these reactions (Blanco et al., 2012; Gaona-Colmán et al., 2017; Mellouki et al., 2003).

Considering the findings mentioned above, it is interesting to analyze the possible effect on k_{OH} when the ether group (R-O) is directly attached to the C=C bond of the unsaturated ketones and the presence of different substituents in the molecule. For this purpose, Table 2 present two basic structures of unsaturated ketones (I and II) and the OH rate coefficients for different unsaturated ketones obtained experimentally and/or estimated using a SAR method (US EPA. Estimation Programs Interface Suite™ for Microsoft® Windows, 2018).

Starting with the less substituted compound, when the substituents *R1, R2,* and *R3* are all hydrogen atoms (3-buten-2-one), a value of k_{OH}= 2 × 10^{-11} cm^3 $molecule^{-1}$ $s^{-1}$was experimentally observed (Holloway et al., 2005). Successive replacement of H atoms with methyl groups, for the positions *R2*(3-penten2-one) and *R3*(4-methyl-3-penten2-one), leads to a considerable increment on the reactivity as shown in Table 2 (Blanco et al., 2012; Gaona-Colmán et al., 2017). Considering the experimental errors of the measurements it is reasonable to conclude that the addition of each methyl group leads to an increase of approximately 4 × 10^{-11} cm^3 $molecule^{-1}$ s^{-1} in the rate coefficient relative to those of basic structure I.

The methyl group added in positions *R2* and *R3* would stabilize the radical formed after the addition of the OH at the C_α for two different effects: (*i*) the positive inductive effect (I+) by the methyl group, which stabilizes the positive charge in the C_β atom and (*ii*) the stabilization due to the hyperconjugation of the carbocation formed at the C_β.

Comparing the experimental value k_{TMBO}= 1.41× $10^{-10}$$cm^3$ $molecule^{-1}$$s^{-1}$obtained in the present work for (*E*)-4-methoxy-3-buten-2-one with its methylated analogue 3-penten-2-one, one can easily realize the increase by a factor of 2 in the rate coefficient when the *R3* substituent is a methoxy group. This can be explained by the oxygen's lone pair of electrons, which delocalizes and increases the electron density within the C=C bond. On

the other hand, the methoxy group is electron withdrawing through a negative inductive effect (I-) via the σ bonds. However, the mesomeric effect is stronger than the inductive one, which is reflected by an increase of the (*E*)-4-methoxy-3-buten-2-one + OH reaction rate coefficient compared to its mono and bi-methylated analogues that can stabilize the corresponding radical structures only by the inductive effect and hyperconjugation, but not by a mesomeric effect.

A similar assessment can be performed considering the basic structure (II). The increasing trend in the reactivity towards OH radicals is quite similar when methyl groups replace H atoms in the structure of 1-pentene-3-one. The experimental rate coefficient k_{MMPO}=3.34× 10^{-10}cm^3 molecule^{-1} s^{-1} obtained in the present work for the reaction of OH radicals with (1*E*)-1-methoxy-2-methyl-1-penten-3-one is quite high but considering the approximate individual contribution of the substituents on the C=C bond as it was assumed previously for the basic structure (I) reflects entirely the system reactivity.

4.1.2Structure-activity relationship (SAR) calculations

In the present work, the AOPWIN software included in the EpiSuite 4.1 was used to estimate the rate coefficients of the structures listed in Table 2(US EPA. Estimation Programs Interface Suite™ for Microsoft® Windows, 2018).

It is worth mentioning that calculated k_{OH} with AOPWIN fit quite well with the experimental values of the simplest structures of the unsaturated ketones shown in Table 2, namely 3-buten-2-one and 1-penten-3-one. However, when the hydrogen atoms are replaced by methyl groups in the C=C system for structures (I) and (II), differences between experimental values and those estimated using SAR method become evident by a factor of 1.2 and 1.5, respectively. For structure (I) with two methyl substituents (4-methyl-3-penten-2-one) the difference remains approximately the same (factor 1.3).

Comparing the kinetic results obtained in this work for MMPO and TMBO with those predicted by AOPWIN, the differences become substantially larger. In Table 2 it can be seen that for k_{TMBO} the results differ by a factor of two and for k_{MMPO} by a factor of three. This fact highlights the limitations of the AOPWIN-SAR method for predicting the specific site for the addition of the OH radical to each carbon atom of an asymmetrical alkene, ignoring a possible stabilization of the reaction intermediate. The stabilization could generate transition states involving the formation of hydrogen bonding complexes between the OH radical and the oxygenated substituents as it was suggested in previous publications (Blanco et al., 2012; Gaona-Colmán et al., 2017; Mellouki et al., 2003).

In conclusion, the AOPWIN-SAR estimation of reaction rate coefficients is a useful tool for simple molecules. However, the OH rate coefficients of the unsaturated ketoethers reported in this work showed significant discrepancies compared with the predicted ones. Probably, as suggested recently by Vereecken et al. (2018) it is not clear if the SAR method can be easily expanded to multifunctional compounds, especially given the small training set available from which to derive cross-substituent parameters or base rate coefficients (Vereecken et al., 2018).

4.2 Reaction product distribution and mechanism

4.2.1(E)-4-methoxy-3-buten-2-one+ OH radicals

Figure 3 shows an IR spectrum recorded before (trace A) UV irradiation applied for a mixture of TMBO and CH_3ONO in air. Trace B shows the spectrum recorded after 10 min of UV irradiation of the reaction mixture. Trace D exhibits the product spectrum after subtraction of not reacted TMBO (from the reference spectra trace C), NO, NO_2, CH_3ONO and H_2O. Traces E, F and G show reference spectra of methyl formate, peroxyacetyl nitrate (PAN) and methyl glyoxal, respectively. Trace H exhibits the

residual product spectrum that is obtained after subtraction of known products from the product spectrum in trace D. The absorption from CO_2 has been removed in all traces for clarity since the band was saturated and no information could be obtained from it accordingly. Methyl formate, peroxyacetyl nitrate, and methyl glyoxal were readily identifiable as reaction products. Concentration−time profiles of TMBO and the identified products, methyl formate, PAN, and methyl glyoxal are shown in Fig.4. The concentration−time distribution supports that methyl formate, methyl glyoxal and PAN are primary reaction products. There is also easily to observe the constant concentrations of TMBO prior to reaction begin. This is accountable for homogeneity of the reaction mixture. Five spectra have been collected before switching on the light which corresponds to 240 s. No decay of TMBO is present in this time suggesting missing dark interference in the reaction system. From Fig. 4 could be observed a conversion of up to 80% of TMBO in 10 min of reaction time.

Depending on the side addition of the OH radical leading to the C_α or C_β, hydroxyalkoxy radicals, A_1 and B_1 will be formed respectively (Scheme 1). Decomposition of the A_1 radical will lead to the formation of methyl formate and methyl glyoxal as primary products. On the other hand, C_3-C_4 bond scission in the B_1 radical will lead to the formation of methyl formate and methyl glyoxal. Additionally, the radical B_1 could decompose through a C_2-C_3 scission generating 2-hydroxy-2-methoxyacetaldehyde and the acetyl radical. This route would, beside the formation of 2-hydroxy-2-methoxyacetaldehyde, be responsible for the primary generation of PAN through further reaction of the acetyl radical with O_2/NO_2. In addition, PAN is known to be formed due to the oxidation of methyl glyoxal (Fischer et al., 2014). The reaction of OH radicals with methyl glyoxal occurs exclusively by abstraction of the aldehydic H atom to form $CH_3C(O)CO$ radicals, which have a very short lifetime, dissociating to form CH_3CO +

CO (Green et al., 1990). Finally, it is expected that acetyl radicals react, in the presence of O_2, with NO_2 to form PAN (Fischer et al., 2014). Acetyl radicals are of particular importance in atmospheric chemistry as they are key contributors to important pollutants in the atmosphere. PAN (peroxyacetyl nitrate), in high NOx environments, is formed exclusively from acetyl peroxy radicals. However, in low NOx environments, acetyl radicals, in the presence of oxygen, generates acetyl peroxy radicals, which further reacts with HO_2 radicals producing $CH_3C(O)OOH$, $CH_3C(O)OH$, O_3 and OH radicals. These secondary products could have a high impact on the atmospheric chemistry on the global scale (Winiberg et al., 2016).

After subtraction of the identified products, the most prominent absorption feature in the IR residual spectra (Fig. 3 trace H) is a carbonyl band at 1730 cm^{-1}, which is more characteristic for an aldehydic than a ketone absorption. This feature suggests the formation of 2-hydroxy-2-methoxyacetaldehyde, which is unfortunately not commercially available. Therefore, direct identification in the residual product spectrum is not possible by using a recorded IR reference spectrum.

Carbonyl absorptions in the IR spectra are present in the 1600-1800 cm^{-1} range and 2-hydroxy-2-methoxyacetaldehyde identification in this region of the IR spectrum is not possible. Beside the parent compound, which is presenting features in this carbonyl absorption specific region, many other products formed during the reaction have absorptions in this range. All the products formed in the reaction system have a specific absorption in the carbonyl range (methylglyoxal, methyl formate, PAN and 2-hydroxy-2-methoxyacetaldehyde). However, the later one must have an important pronounced peak in the O-H absorption area; therefore, we may assume the unique absorption at 3550 cm^{-1} as being attributed to the O-H absorption of 2-hydroxy-2-methoxyacetaldehyde (SI

Fig.S1). This is a strong indication of the 2-hydroxy-2-methoxyacetaldehyde formation, which is in agreement with the proposed mechanism in Scheme 1.

Plots of the concentrations of the carbonyls formed vs reacted TMBO give molar formation yields of (65 ± 12) % for methyl formate, (56 ± 16) % for PAN and (69 ± 14) % for methyl glyoxal. The yields have been corrected for secondary reactions with OH radicals as well as for the photolysis and wall deposition processes where necessary (Tuazon et al., 1986). Exemplary plots for the product formation yields are shown in the SI Fig. S2.

4.2.2(1*E*)-1-methoxy-2-methyl-1-penten-3-one+ *OH radicals*

Figure 5, trace A shows the infrared spectrum for an initial reaction mixture of a MMPO/CH_3ONO/air mixture prior to irradiation; trace B exhibits the spectrum recorded after 10 min of irradiation and hence the occurring reaction; trace C shows a reference spectrum of MMPO recorded in a separate experiment in air at 1 atm and 298 K; trace D shows the product spectrum recorded after 10 min of irradiation and after subtraction of not reacted MMPO as well as subtraction of CH_3ONO, NO, H_2O and NO_2 absorption bands; trace E shows a reference spectrum of methyl formate; trace F a reference spectrum of 2,3-pentanedione and trace G a reference spectrum of peroxypropionyl nitrate (PPN). Trace H shows the residual product spectrum after subtraction of the identified reaction products in trace D.

The absorption from CO_2 has been removed in all traces for clarity since the band was saturated and no additional information could be obtained, accordingly. Methyl formate and peroxypropionyl nitrate were identified as reaction products. Concentration−time profiles of MMPO, methyl formate and peroxypropionyl nitrate are shown in Fig.6. Figure 6 supports that methyl formate and peroxypropionyl nitrate are primary reaction

products. MMPO concentration is constant during 5 spectra recorded in dark which consist of 120 s mixing time. Perfect homogeneity and no dark interferences could be observed. From Fig. 6 could be observed a total conversion of MMPO in 10 min of reaction time.

After the addition of the OH radical to the double bond of MMPO and subsequent addition of an oxygen molecule followed by reaction with NO, two different hydroxyalkoxy radicals, A_2 and B_2 (scheme 2) could be generated. Unlike for TMBO, the reaction of MMPO with OH radicals at the C_β position could lead to the formation of the more stable tertiary radical A_2 due to the presence of a methyl group in the α position to the carbonyl group.

Scheme 2 shows that both addition channels would lead to the formation of methyl formate and 2,3-pentanedione if the hydroxyalkoxy radical would follow dissociation of bond I in the A_2 radical intermediate and the dissociation of bond II in the B_2 radical intermediate.

The hydroxyalkoxy radical B_2 could lead, beside the formation of 2,3-pentanedione and methyl formate by following scission of bond II, to the formation of 2-hydroxy-2-methyl-3-oxopentanal as product and formaldehyde as reaction co-product as a result of the decomposition of the B2 radical from scission of bond I. Formaldehyde could not be identified as reaction product since it is formed from CH_3ONO photolysis and is present in the reaction spectra. 2-hydroxy-2-methyl-3-oxopentanal is not commercially available and in the absence of a mass spectrometry technique, which could at least identify the mass of this product there, its formation is only an assumption.

Decomposition channel for the A2 radical could follow route I leading to the formation of 2,3-pentanedione and the radical CH_3OCHOH, which could further, in the presence of oxygen, form methyl formate as a co-product. Figure 5 trace E shows a reference

spectrum of methyl formate. The absorption bands at 1210 cm^{-1} and 1755 cm^{-1} were used to identify and quantify the formation of methyl formate.

The formation of 2,3-pentanedioneis confirmed qualitatively by comparison of the product spectrum (Fig.5 trace D) with the existing reference spectrum (Fig.5, trace F). Although there is no doubt in the formation of 2,3-pentanedione, the partial or total overlap of the low intensity absorption bands did not allow us to perform reliable subtraction results to proceed for its quantification. 2,3-pentanedione exists predominantly in the keto form with the enol form being present to a few percent, at the most, in the gas phase at room temperature (Kung, 1974; Szabó et al., 2011). The predominance of the keto form for this compound makes its reactivity toward OH radicals much lower. Furthermore, in comparison with 2,4-pentanedione, a dicarbonyl compound having the enolic form predominantly and thus being more reactive toward OH radicals (9.05×10^{-11} cm^3 $molecule^{-1}$ s^1) (Zhou et al., 2008), 2,3-pentanedione, with a rate coefficient for the reaction with OH radicals of 2.25×10^{-12} cm^3 $molecule^{-1}$ s^1 (Szabó et al., 2011) is 40 times less reactive and consequently the secondary reaction with OH radicals could be of less importance (Messaadia et al., 2015).

On the other hand, photolysis quantum yields for 2,3-pentanedione using XeF laser radiation and UV lamps at room temperature in 1000 mbar of air were studied by Szabó et al., 2011. The results obtained in their work suggest that 2,3-pentanedione would suffer significant photochemical changes even at relatively long wavelengths involving short photolysis lifetime in the troposphere. If we consider these facts, it would be possible to expect a non-negligible photolysis of the compound in our experimental system under the conditions used for this study.

Decomposition of the A2 hydroxyalkoxy radical could follow the scission on route II leading to 1-hydroxy-1-methoxypropan-2-one and propionyl radical. 1-hydroxy-1-

methoxypropan-2-oneis not commercially available and thus is not possible to identify this compound by comparison with an infrared reference spectrum. However, the absorption band with the maximum at 3512 cm^{-1} could be assumed to the OH stretching band of 1-hydroxy-1-methoxypropan-2-one (see SI Fig.S3). The infrared spectrum in Fig.S3 presents one main absorption feature that could be attributed to the O-H stretching of 1-hydroxy-1-methoxypropan-2-one produced by the more stable tertiary radical (A_2). The propionyl radical could further form peroxypropionyl nitrate (PPN) (Fig. 5 trace G) in the presence of O_2 and NO_2.

Plots of the concentrations of methyl formate and PPN formed against reacted MMPO in the OH radical reaction give molar formation yields of (40 ± 12)% and (17 ± 6) % respectively. The yields have been corrected for secondary reactions with OH radicals using the method outlined by Tuazón et al., 1986. Exemplary plots of the product formation yields are shown in the SI Fig. S4.

5. Atmospheric Implications and Conclusions

Once emitted into the atmosphere, it is expected that unsaturated ketoethers such as TMBO and MMPO will follow gas phase degradation processes initiated by the main tropospheric oxidants (OH radicals, ozone, chlorine atoms and NO_3 radicals). Rate coefficients obtained in this work for the reaction of TMBO and MMPO with OH radicals were used to calculate their tropospheric lifetimes using the expression $\tau_x=1/k_{ox}[Ox]$ where [Ox] is the typical atmospheric concentration of the oxidant in the troposphere and k_{ox} is the rate coefficient for the reaction of the TMBO and MMPO towards the oxidants. Considering 12-h day-time average OH radical concentration of 2×10^6 molecule cm^{-3} (global weighted-average concentration) (Bloss et al., 2005) an average lifetime of 0.98 and 0.42 hours were estimated for TMBO and MMPO, respectively. As mentioned

before, in the literature there is only one experimental determination for the TMBO reaction rate coefficient with O_3 performed by Grosjean et al. (1999). By using k_{O3}=1.3 × 10^{-16} cm^3 $molecule^{-1}$ $s^{-1}$and a 24-h average O_3 concentration of 7×10^{11} molecule cm^{-3} (Logan, 1985) an estimated tropospheric residence time of 3.1 hours was calculated. A similar tropospheric lifetime is expected for MMPO towards ozone but due to the lack of kinetic data, no exact value could be calculated for MMPO. Unfortunately, no kinetic data are available for the reactions of TMBO and MMPO with Cl atoms and NO_3 radicals. However, it is reasonable to conclude that reaction with OH radicals is the main tropospheric removal pathway during daytime for the two ketoethers studied due to the short lifetimes calculated in this work. For ethers it is known that photodissociation quantum yields are relatively low and the photolysis of ketones becomes important only at high altitudes (Mellouki et al., 2015). Thus, it is reasonable to assume that photolysis of the studied compounds is only of minor importance for their atmospheric removal.

The reaction products of the OH radical initiated degradation of MMPO and TMBO confirm that the main degradation mechanisms follow the addition pathways to the double bonds. Products, identified and quantified from these reactions, are carbonyls like methyl formate, methyl glyoxal and 2,3-pentanedione and long-lived nitrogen containing compounds such as PAN and PPN. Both type of these oxygenated products could have further impact on atmospheric processes. The present study proposes new gas phase contributors to the total budget of methyl glyoxal in the atmosphere a well known precursor for SOAs formation (Fu et al., 2008). Even more this study becomes important since MMPO and TMBO are VOCs possibly released from open biomass burning events whose emissions factors for methyl glyoxal are not well established (Zarzana et al., 2018). PAN and PPN, quantified also as reaction products, are phytotoxic air pollutants, which act as NOx reservoir in remote areas (Taylor, 1969). Beside a large number of PAN

measurement campaigns, most recent chemical transport models still unsolved the PANs global distributions due to the lack of understanding of the PAN source attribution in the atmosphere (Fischer et al., 2014). Although the acetyl radical is intermediary in the formation of PAN in this study, by its acetyl peroxy radical formed in the presence of oxygen, this radical it could play an important role in the HO_x balance over the low NO_x environment. The acetyl peroxy radical is a well known precursor of OH radicals as a result of the reaction with HO_2 in the remote atmosphere (Winiberg et al., 2016). Therefore, the gas phase mechanism proposed in this study could be of importance for understanding atmospheric processes at the global scale, either in the atmosphere with low NO_x levels or in the atmosphere with increased NO_x. The results of the present study provide improved insights regarding the important contribution of multifunctional VOCs in the chemistry of atmosphere.

6. Competing interests

The authors declare that they have no conflict of interest.

7. Author contribution

RG, IB, IGB, PW designed experimental setup, RG conducted the measurements, RG and IGB processed the data, RG, IGB and PW prepared the manuscript with contribution from all the co-authors on different stages of writing process.

8. Acknowledgements

R. Gibilisco acknowledges the Alexander von Humboldt foundation for providing a Georg Forster postdoctoral fellowship. The authors acknowledge financial support from the European grant EUROCHAMP-2020 and the Deutsche Forschungsgemeinschaft (DFG). I. Bejan acknowledges the UEFISCDI grant PN-III-P4-ID-PCE-2016-0807.

9. References

Atkinson, R.: Atmospheric chemistry of VOCs and NO(x), Atmos. Environ., 34(12–14), 2063–2101, doi:10.1016/S1352-2310(99)00460-4, 2000.

Atkinson, R. and Aschmann, S. M.: Rate constants for the reaction of OH radicals with a series of alkenes and dialkenes at 295 ± 1 K, Int. J. Chem. Kinet., 16(10), 1175–1186, doi:10.1002/kin.550161002, 1984.

Atkinson, R., Baulch, D. L., Cox, R. A., Crowley, J. N., Hampson, R. F., Hynes, R. G., Jenkin, M. E., Rossi, M. J. and Troe, J.: Atmospheric Chemistry and Physics Evaluated kinetic and photochemical data for atmospheric chemistry: Volume II-gas phase reactions of organic species The IUPAC Subcommittee on Gas Kinetic Data Evaluation for Atmospheric Chemistry. [online] Available from: www.atmos-chem-phys.net/6/3625/2006/ (Accessed 28 August 2019), 2006.

Blanco, M. B. and Teruel, M. A.: Atmospheric photodegradation of ethyl vinyl ketone and vinyl propionate initiated by OH radicals, Chem. Phys. Lett., 502,(4–6), 159–162, doi:10.1016/j.cplett.2010.12.059, 2011.

Blanco, M. B., Barnes, I. and Wiesen, P.: Kinetic investigation of the OH radical and Cl atom initiated degradation of unsaturated ketones at atmospheric pressure and 298 K, J. Phys. Chem. A, 116(24), 6033–6040, doi:10.1021/jp2109972, 2012.

Bloss, W. J., Evans, M. J., Lee, J. D., Sommariva, R., Heard, D. E. and Pilling, M. J.: The oxidative capacity of the troposphere: Coupling of field measurements of OH and a global chemistry transport model, Faraday Discuss., 130, 425–436, doi:10.1039/b419090d, 2005.

Calvert, J.G., Orlando, J.J., Stockwell, W.R. and Wallington, T. J.: The Mechanisms of Reactions Infuencing Atmospheric Ozone, Oxford University Press., 2015.

Calvert, J., Mellouki, A., Orlando, J. J., Pilling, M. J. . and Wallington, T. J.: The Mechanisms of Atmospheric Oxidation of the Oxygenates, Oxford University Press, New York., 2011.

Cilek, J. E., Ikediobi, C. O., Hallmon, C. F., Johnson, R., Onyeozili, E. N., Farah, S. M., Mazu, T., Latinwo, L. M., Ayuk-Takem, L. and Berniers, U. R.: Semi-field evaluation of several novel alkenol analogs of 1-octen-3-ol as attractants to adult Aedes albopictus

and Culex quinquefasciatus., J. Am. Mosq. Control Assoc., 27(3), 256–262, doi:10.2987/10-6097.1, 2011.

Fischer, E. V., Jacob, D. J., Yantosca, R. M., Sulprizio, M. P., Millet, D. B., Mao, J., Paulot, F., Singh, H. B., Roiger, A., Ries, L., Talbot, R. W., Dzepina, K. and Pandey Deolal, S.: Atmospheric peroxyacetyl nitrate (PAN): A global budget and source attribution, Atmos. Chem. Phys., 14(5), 2679–2698, doi:10.5194/acp-14-2679-2014, 2014.

Fu, T. M., Jacob, D. J., Wittrock, F., Burrows, J. P., Vrekoussis, M. and Henze, D. K.: Global budgets of atmospheric glyoxal and methylglyoxal, and implications for formation of secondary organic aerosols, J. Geophys. Res. Atmos., 113, D15, doi:10.1029/2007JD009505, 2008.

Gaona-Colmán, E., Blanco, M. B. and Teruel, M. A.: Kinetics and product identification of the reactions of (*E*)-2-hexenyl acetate and 4-methyl-3-penten-2-one with OH radicals and Cl atoms at 298 K and atmospheric pressure, Atmos. Environ., 161, 155–166, doi:10.1016/j.atmosenv.2017.04.033, 2017.

Gøgsig, T. M., Nielsen, D. U., Lindhardt, A. T. and Skrydstrup, T.: Palladium catalyzed carbonylative Heck reaction affording monoprotected 1,3-ketoaldehydes, Org. Lett., 14(10), 2536–2539, doi:10.1021/ol300837d, 2012.

Green, M., Yarwood, G. and Niki, H.: FTIR study of the Cl-atom initiated oxidation of methylglyoxal, Int. J. Chem. Kinet., 22(7), 689–699, doi:10.1002/kin.550220705, 1990.

Grosjean, E. and Grosjean, D.: The reaction of unsaturated aliphatic oxygenates with ozone, J. Atmos. Chem., 32(2), 205–232, doi:10.1023/A:1006122000643, 1999.

Hatch, L. E., Luo, W., Pankow, J. F., Yokelson, R. J., Stockwell, C. E. and Barsanti, K. C.: Identification and quantification of gaseous organic compounds emitted from biomass burning using two-dimensional gas chromatography-time-of-flight mass spectrometry, Atmos. Chem. Phys., 15(4), 1865–1899, doi:10.5194/acp-15-1865-2015, 2015.

Holloway, A. L., Treacy, J., Sidebottom, H., Mellouki, A., Daële, V., Le Bras, G. and Barnes, I.: Rate coefficients for the reactions of OH radicals with the keto/enol tautomers of 2,4-pentanedione and 3-methyl-2,4-pentanedione, allyl alcohol and methyl vinyl ketone using the enols and methyl nitrite as photolytic sources of OH, J. Photochem. Photobiol. A Chem., 176(1-3 SPEC. ISS.), 183–190, doi:10.1016/j.jphotochem.2005.08.031, 2005.

Jiménez, E., Cabañas, B. and Lefebvre, G.: Environment, Energy and Climate Change I, in The Handbook of Environmental Chemistry, Springer., 2014.

Kumar, N. R., Poornachandra, Y., Swaroop, D. K., Dev, G. J., Kumar, C. G. and Narsaiah, B.: Synthesis of novel ethyl 2,4-disubstituted 8-(trifluoromethyl)pyrido[2',3':3,4]pyrazolo[1,5-a]pyrimidine-9-carboxylate derivatives as promising anticancer agents., Bioorg. Med. Chem. Lett., 26(21), 5203–5206, 2016.

Kung, J. T.: New caramel compound from coffee, J. Agric. Food Chem., 22(3), 494–496, 1974.

Li, M., Liu, Y. and Wang, L.: Gas-phase ozonolysis of furans, methylfurans, and

dimethylfurans in the atmosphere, Phys. Chem. Chem. Phys., 20(38), 24735–24743, doi:10.1039/c8cp04947e, 2018.

Logan, J. A.: Tropospheric ozone: seasonal behavior, trends, and anthropogenic influence., J. Geophys. Res., 90(D6), 10463–10482, doi:10.1029/JD090iD06p10463, 1985.

Lv, C., Du, L., Tsona, N., Jiang, X. and Wang, W.: Atmospheric Chemistry of 2-Methoxypropene and 2-Ethoxypropene: Kinetics and Mechanism Study of Reactions with Ozone, Atmosphere (Basel)., 9(10), 401, 2018.

Mellouki, A., Le Bras, G. and Sidebottom, H.: Kinetics and Mechanisms of the Oxidation of Oxygenated Organic Compounds in the Gas Phase, Chem. Rev., 103(12), 5077–5096, doi:10.1021/cr020526x, 2003.

Mellouki, A., Wallington, T. J. and Chen, J.: Atmospheric Chemistry of Oxygenated Volatile Organic Compounds: Impacts on Air Quality and Climate, Chem. Rev., 115(10), 3984–4014, doi:10.1021/cr500549n, 2015.

Messaadia, L., El Dib, G., Ferhati, A. and Chakir, A.: UV-visible spectra and gas-phase rate coefficients for the reaction of 2,3-pentanedione and 2,4-pentanedione with OH radicals, Chem. Phys. Lett., 626, 73–79, doi:10.1016/j.cplett.2015.02.032, 2015.

Szabó, E., Djehiche, M., Riva, M., Fittschen, C., Coddeville, P., Sarzyński, D., Tomas, A. and Dóbé, S.: Atmospheric chemistry of 2,3-pentanedione: Photolysis and reaction with OH radicals, J. Phys. Chem. A, 115(33), 9160–9168, doi:10.1021/jp205595c, 2011.

Taylor, O. C.: Importance of peroxyacetyl nitrate (pan) as a phytotoxic air pollutant, J. Air Pollut. Control Assoc., 19(5), 347–351, doi:10.1080/00022470.1969.10466498, 1969.

Taylor, W. D., Allston, T. D., Moscato, M. J., Fazekas, G. B., Kozlowski, R. and Takacs, G. A.: Atmospheric photodissociation lifetimes for nitromethane, methyl nitrite, and methyl nitrate, Int. J. Chem. Kinet., 12(4), 231–240, doi:10.1002/kin.550120404, 1980.

Tuazon, E. C., Leod, H. Mac, Atkinson, R. and Carter, W. P.: α-Dicarbonyl Yields from the NOx-Air Photooxidations of a Series of Aromatic Hydrocarbons in Air, Environ. Sci. Technol., 20(4), 383–387, doi:10.1021/es00146a010, 1986.

US EPA. Estimation Programs Interface Suite™ for Microsoft® Windows, v 4. 11. E. P. A.: AOPWIN, 2018.

Vereecken, L., Aumont, B., Barnes, I., Bozzelli, J. W., Goldman, M. J., Green, W. H., Madronich, S., Mcgillen, M. R., Mellouki, A., Orlando, J. J., Picquet-Varrault, B., Rickard, A. R., Stockwell, W. R., Wallington, T. J. and Carter, W. P. L.: Perspective on Mechanism Development and Structure-Activity Relationships for Gas-Phase Atmospheric Chemistry, Int. J. Chem. Kinet., 50(6), 435–469, doi:10.1002/kin.21172, 2018.

Villanueva, F., Cabañas, B., Monedero, E., Salgado, S., Bejan, I. and Martin, P.: Atmospheric degradation of alkylfurans with chlorine atoms: Product and mechanistic study, Atmos. Environ., 43(17), 2804–2813, doi:10.1016/j.atmosenv.2009.02.030, 2009.

Winiberg, F. A. F., Dillon, T. J., Orr, S. C., Groß, C. B. M., Bejan, I., Brumby, C. A., Evans, M. J., Smith, S. C., Heard, D. E. and Seakins, P. W.: Direct measurements of OH and other product yields from the HO2 + CH3C(O)O2 reaction, Atmos. Chem. Phys., 16(6), 4023–4042, doi:10.5194/acp-16-4023-2016, 2016.

Zarzana, K. J., Selimovic, V., Koss, A. R., Sekimoto, K., Coggon, M. M., Yuan, B., Dubé, W. P., Yokelson, R. J., Warneke, C., De Gouw, J. A., Roberts, J. M. and Brown, S. S.: Primary emissions of glyoxal and methylglyoxal from laboratory measurements of open biomass burning, Atmos. Chem. Phys., 18(20), 15451–15470, doi:10.5194/acp-18-15451-2018, 2018.

Zhou, S., Barnes, I., Zhu, T., Klotz, B., Albu, M., Bejan, I. and Benter, T.: Product study of the OH, NO3, and O3 initiated atmospheric photooxidation of propyl vinyl ether, Environ. Sci. Technol., 40(17), 5415–5421, doi:10.1021/es0605422, 2006.

Zhou, S., Barnes, I., Zhu, T., Bejan, I., Albu, M. and Benter, T.: Atmospheric chemistry of acetylacetone, Environ. Sci. Technol., 42(21), 7905–7910, doi:10.1021/es8010282, 2008.

Figure Captions

Figure 1: Relative rate data for the reaction of OH radicals with (*E*)-4-methoxy-3-buten-2-one using propene (■) and isobutene (●) as reference compounds at 298 K and atmospheric pressure of air.

Figure 2: Relative rate data for the reaction of OH radicals with (1*E*)-1-methoxy-2-methyl-1-penten-3-one using propene (■) and isobutene (●) as reference compounds at 298 K and atmospheric pressure of air.

Figure 3: Infrared spectral data: trace A infrared spectrum of a TMBO/CH_3ONO/air reaction mixture before irradiation; trace B mixture after 10 min irradiation; trace C reference spectrum of TMBO; trace D product spectrum; trace E reference spectrum of methyl formate; trace F reference spectrum of peroxyacetyl nitrate; trace G reference spectrum of methyl glyoxal; trace H residual spectrum after subtraction of the identified reaction products in trace D.

Figure 4: Concentration−time dependencies for the reaction of TMBO (■) + OH radicals and the quantified products, methyl formate (♦MF), peroxyacetyl nitrate (●PAN), and methyl glyoxal (▲MG).

Figure 5: Infrared spectral data: trace A infrared spectrum of a MMPO/CH_3ONO/air reaction mixture before irradiation; trace Bmixture after 10 min irradiation; trace C reference spectrum of MMPO; traced product spectrum; trace E reference spectrum of methyl formate; trace F reference spectrum of 2, 3-pentanedione; trace G reference spectrum of PPN; trace H residual spectrum after subtraction of the identified reaction products in trace D.

Figure 6: Concentration−time profiles for the reaction of MMPO (■)+ OH radicals and the quantified product methyl formate (♦MF) and peroxypropionyl nitrate (●PPN).

Table 1. Rate coefficient ratios $k_{UKE}/k_{Reference}$ and rate coefficients for the reaction of OH radicals with (*E*)-4-methoxy-3-buten-2-one and (1*E*)-1-methoxy-2-methyl-1-penten-3-one at (298 ± 3) K in 1 atm of air.

Compound	Reference	$k_{UKE}/k_{Reference}$	k_{UKE} (10^{-10} cm^3 molecule^{-1}s^{-1})
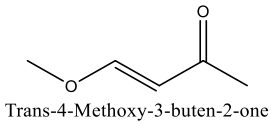 Trans-4-Methoxy-3-buten-2-one	Isobutene	2.41 ± 0.02	1.26 ± 0.06
	Isobutene	2.74 ± 0.04	1.43 ± 0.07
	Isobutene	2.67 ± 0.09	1.40 ± 0.10
	Propene	5.02 ± 0.06	1.46 ± 0.05
	Propene	5.20 ± 0.07	1.51 ± 0.06
	Average		**1.41 ± 0.11**
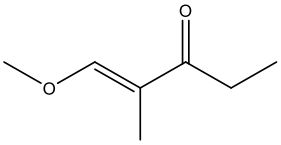 (E)-1-methoxy-2-methyl-1-penten-3-one	Isobutene	6.30± 0.12	3.30 ± 0.16
	Isobutene	6.54± 0.38	3.42 ± 0.25
	Propene	11.00 ± 0.77	3.19 ± 0.25
	Propene	11.88 ± 0.49	3.45 ± 0.19
	Average		**3.34 ± 0.43**

Table 2. OH rate coefficients for different unsaturated ketones obtained experimentally and predicted using a SAR method.

Basic structure	***Substituent -R***	***Compound name***	***Experimental*** k_{OH} **(cm^3 $molecule^{-1}s^{-1}$)**	***SAR calculated*** k_{OH}[f] **(cm^3 $molecule^{-1}s^{-1}$)**
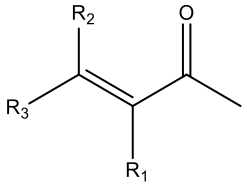 (I)	$R_1=R_2=R_3=H$	3-buten-2-one	$(2.0 \pm 0.3) \times 10^{-11}$[a]	$H_{abs}= 1.02 \times 10^{-13}$ $OH_{Add}= 2.37 \times 10^{-11}$ **Overall= 2.38×10^{-11}**
	$R_1=H$, $R_2=H$, $R_3=CH_3$	3-penten-2-one	$(7.22 \pm 1.74) \times 10^{-11}$[b]	*(E)-isomer* $H_{abs}= 2.38 \times 10^{-13}$ $OH_{Add}= 5.76 \times 10^{-11}$ **Overall=5.78×10^{-11}**
	$R_1=H$, $R_2=CH_3$, $R_3=CH_3$	4-methyl-3-penten-2-one	$(1.02 \pm 0.20) \times 10^{-10}$[c]	$H_{abs}=3.74 \times 10^{-13}$ $OH_{Add}= 7.82\times 10^{-11}$ **Overall=7.86×10^{-11}**
	$R_1=H$, $R_2=H$, $R_3=OCH_3$	(*E*)-4-methoxy-3-buten-2-one	$(1.41 \pm 0.11) \times 10^{-10}$[d]	$H_{abs}=9.32 \times 10^{-13}$ $OH_{Add}= 7.49 \times 10^{-11}$ **Overall=7.58×10^{-11}**
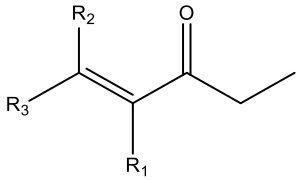 (II)	$R_1=R_2=R_3=H$	1-penten-3-one	$(2.90 \pm 0.79) \times 10^{-11}$[e]	$H_{abs}=1.23 \times 10^{-12}$ $OH_{Add}= 2.37 \times 10^{-11}$ **Overall=2.49×10^{-11}**
	$R_1=H$, $R_2=H$, $R_3=CH_3$	(*E*)-4-hexen-3-one	$(9.04 \pm 2.12) \times 10^{-11}$[b]	*(E)-isomer* $H_{abs}=1.37 \times 10^{-12}$ $OH_{Add}= 5.76\times 10^{-11}$ **Overall=5.90×10^{-11}**
	$R_1=H$, $R_2=CH_3$, $R_3=CH_3$	5-methyl-4-hexen-3-one	-	$H_{abs}=1.50 \times 10^{-12}$ $OH_{Add}=7.82 \times 10^{-11}$ **Overall=7.97×10^{-11}**
	$R_1=CH_3$, $R_2=H$, $R_3=OCH_3$	(1*E*)-1-methoxy-2-methyl-1-penten-3-one	$(3.34 \pm 0.43) \times 10^{-10}$[d]	$H_{abs}= 2.20 \times 10^{-12}$ $OH_{Add}= 1.02 \times 10^{-10}$ **Overall=1.04×10^{-10}**

a-(Holloway et al., 2005); b-(Blanco et al., 2012); c-(Gaona-Colmán et al., 2017); d- This work; e-(Blanco and Teruel, 2011)

Scheme 1. Simplified reaction mechanism for the addition channel in the OH-radical initiated oxidation of the(*E*)-4-methoxy-3-buten-2-one. Quantified products appear in the boxes and the identified products are rounded by a dashed rectangle.

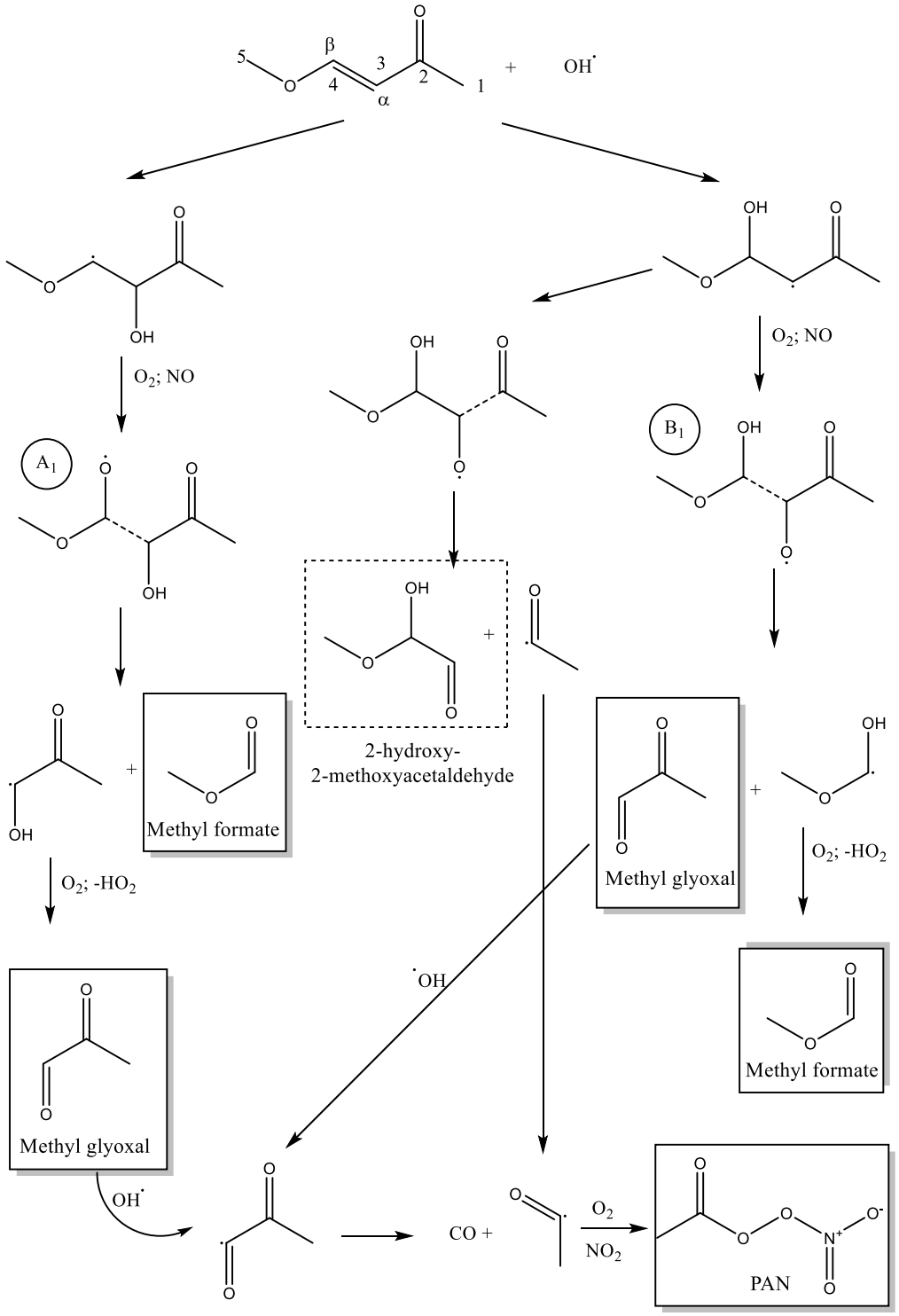

Scheme 2. Simplified reaction mechanism for the addition channel in the OH-radical initiated oxidation of (1*E*)-1-methoxy-2-methyl-1-penten-3-one.Quantified products appear in the boxes and the identified products are rounded by a dashed rectangle.

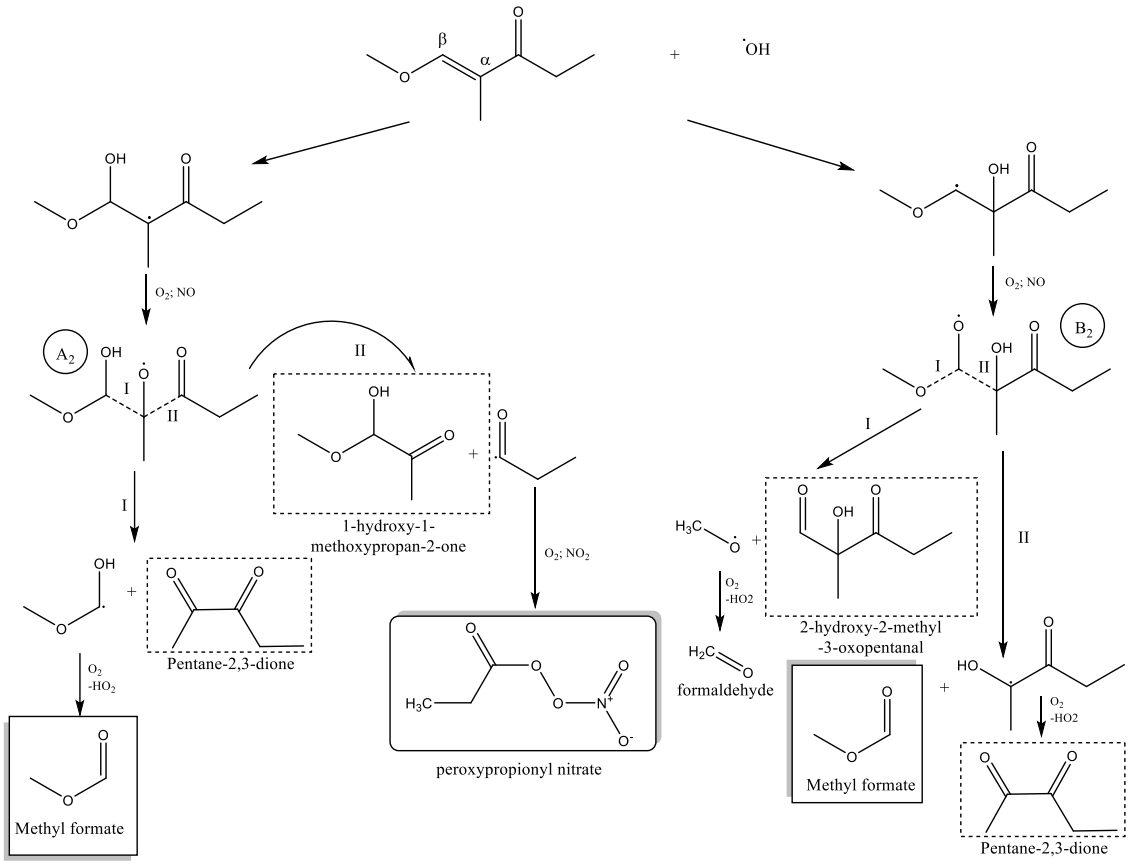

Fig. 1

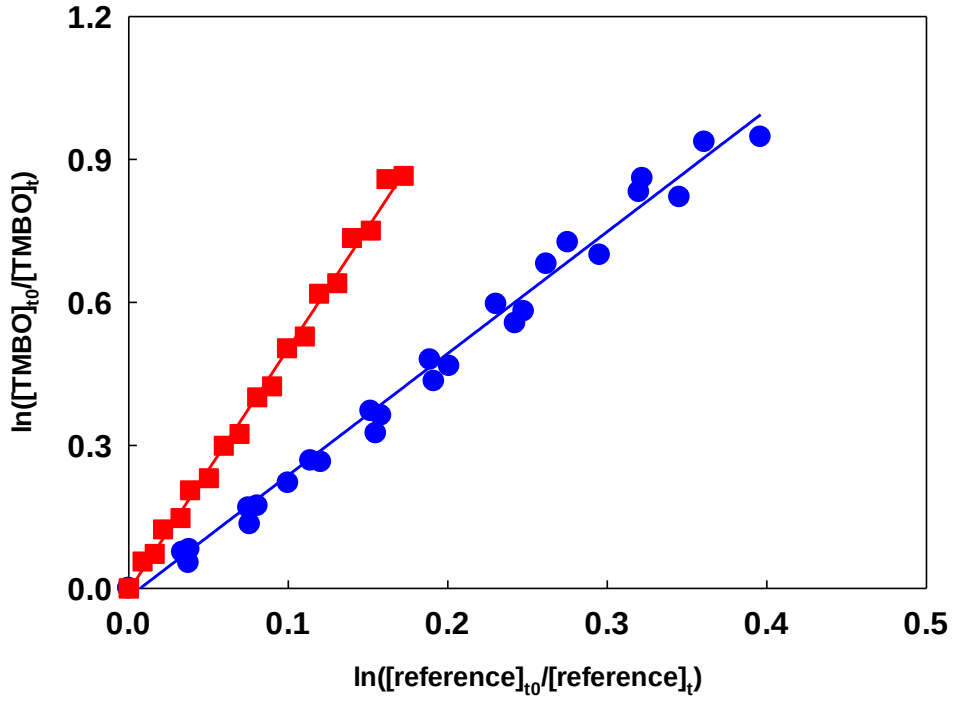
1.2
0.9
0.6
0.3
0.0
0.0
0.1
0.2
0.3
0.4
0.5
ln([TMBO]t0/[TMBO]t)
ln([reference]t0/[reference]t)

Fig.2

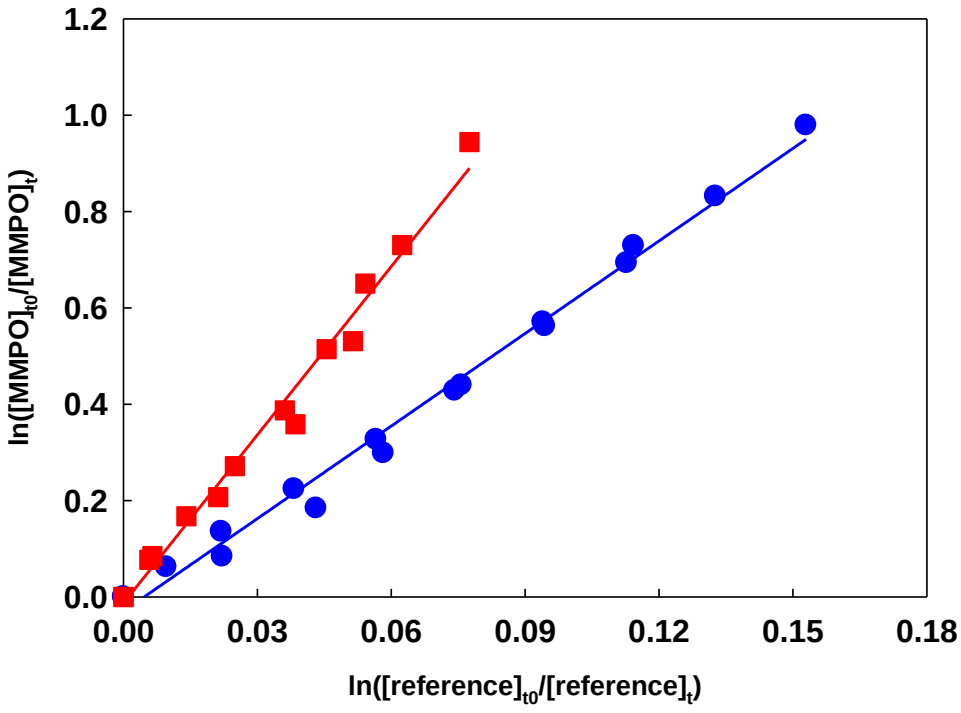
1.2
1.0
0.8
0.6
0.4
0.2
0.0
0.00
0.03
0.06
0.09
0.12
0.15
0.18
ln([MMPO]t0/[MMPO]t)
ln([reference]t0/[reference]t)

Fig. 3

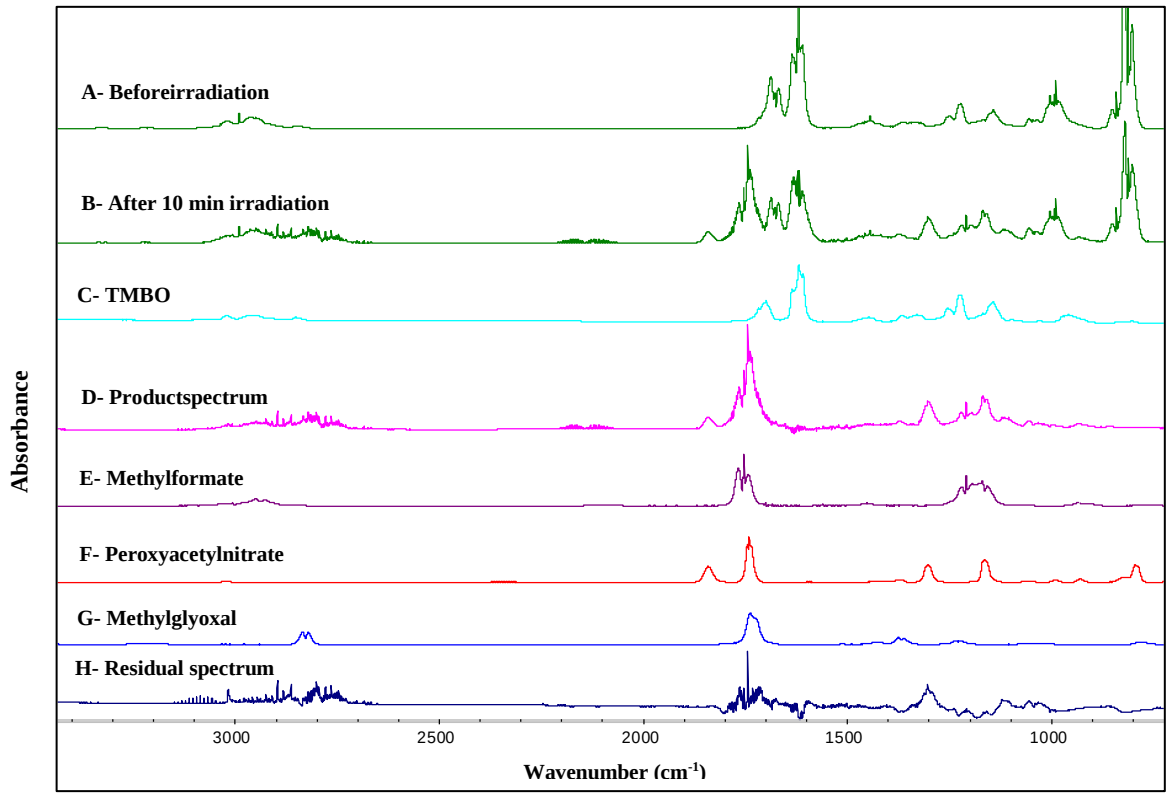
A- Beforeirradiation
B- After 10 min irradiation
C- TMBO
D- Productspectrum
E- Methylformate
F- Peroxyacetylnitrate
G- Methylglyoxal
H- Residual spectrum
Absorbance
3000
2500
2000
1500
1000
Wavenumber (cm-1)

Fig. 4

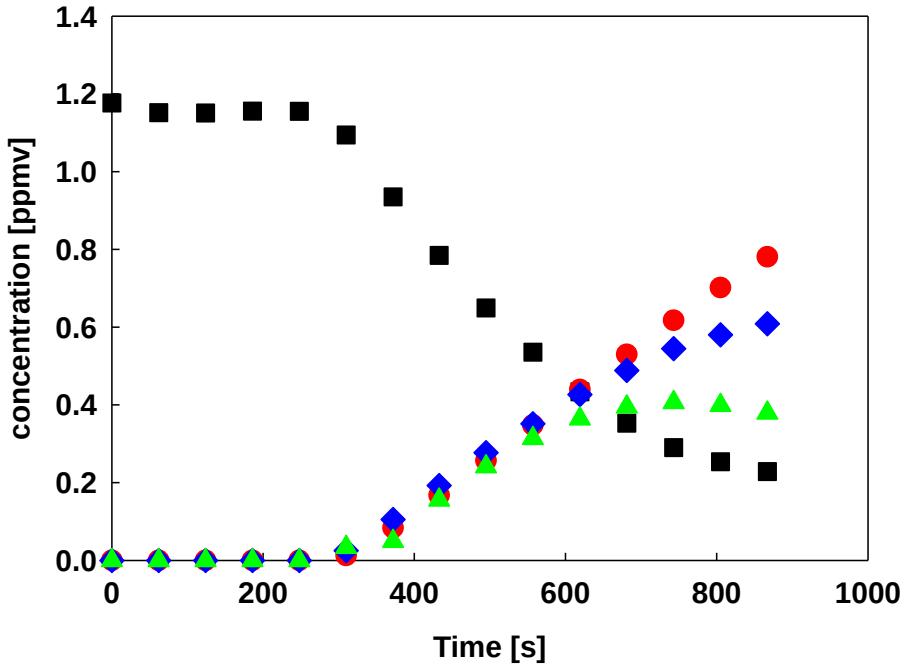
concentration [ppmv]
1.4
1.2
1.0
0.8
0.6
0.4
0.2
0.0
0
200
400
600
800
1000
Time [s]

Fig. 5

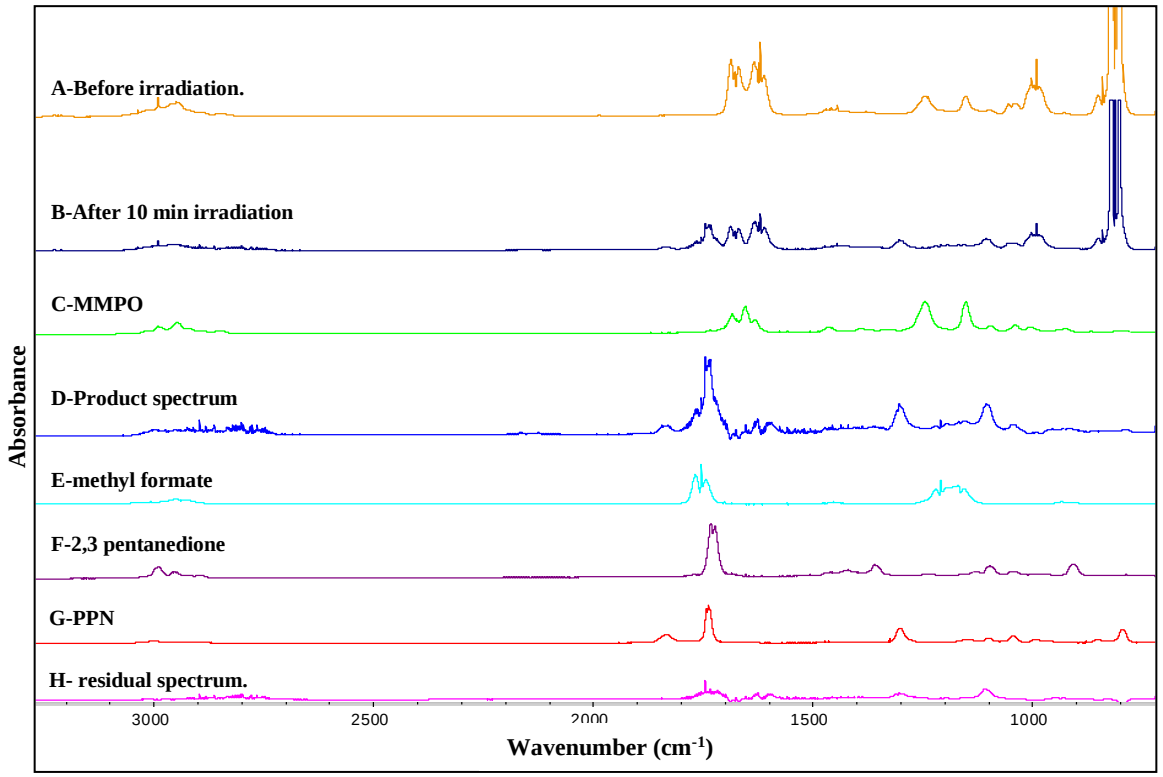
A-Before irradiation.
B-After 10 min irradiation
C-MMPO
D-Product spectrum
E-methyl formate
F-2,3 pentanedione
G-PPN
H- residual spectrum.
Absorbance
3000
2500
2000
1500
1000
Wavenumber (cm-1)

Fig. 6

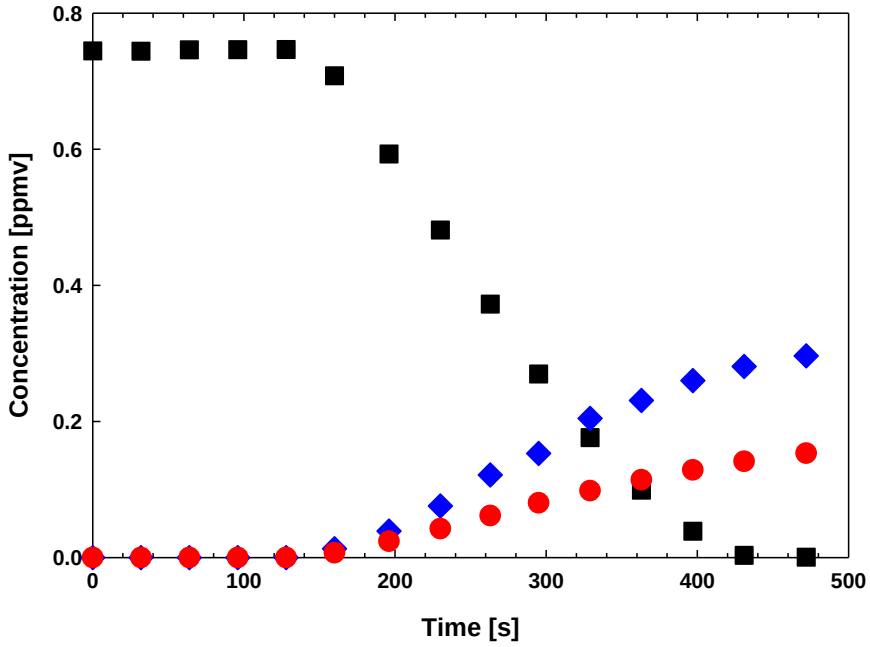
0.8
0.6
0.4
0.2
0.0
Concentration [ppmv]
0
100
200
300
400
500
Time [s]